Effects of Systematic Methyl Substitution of Metal (III) Tris(*n*-Methyl-8-Quinolinolato) Chelates on Material Properties for Optimum Electroluminescence Device Performance

Linda S. Sapochak,*,† Asanga Padmaperuma,† Nancy Washton,† Flocerfida Endrino,† Gregory T. Schmett,† Jeffrey Marshall,† Daniel Fogarty,† Paul E. Burrows,‡,§ and Stephen R. Forrest‡

Contribution from the Department of Chemistry, University of Nevada, Las Vegas, Nevada 89154-4003, and Department of Electrical Engineering, Princeton University, Princeton, New Jersey 08544

Received January 16, 2001

Abstract: We relate the chemical structure of a series of methyl (Me) substituted group III metal tris(8-quinolinolato) chelates (nMeq$_3$M: n = 0, 3, 4, 5; M = Al^{3+}, Ga^{3+}) to their photoluminescence (PL), electroluminescence, and thermal properties. Methylation of the 8-quinolinol ligand at the 3 or 4 position (pyridyl ring) results in a factor of 1.4 and 3.0 enhancement of PL quantum efficiency (ϕ_{PL}), respectively, whereas methylation at the 5 position (phenoxide ring) results in a factor of ∼3.0 decrease in ϕ_{PL} relative to the unsubstituted analogue. Electroluminescent quantum efficiencies of undoped organic light-emitting devices using the aluminum tris(8-quinolinolato) chelates are 1, 0.45, 1.4, and 0.80% for unsubstituted 5-, 4-, and 3-methyl-8-quinolinol ligands, respectively. Devices made with the latter two ligands have a higher operating voltage to generate the same current density. Similar trends were observed for methylation of gallium tris(8-quinolinolato) chelates. We relate these results to the thermal properties of the compounds measured by simultaneous differential scanning calorimetry and thermal gravimetric analysis. The C-4 methylated derivatives exhibit ∼60 °C lower crystalline melting points than all other derivatives, indicating the weakest cohesive forces between molecules. Unlike Alq$_3$, both the C-4 and C-5 methylated derivatives show no recrystallization of the glassy state below 500 °C and exhibit ∼20−25 °C higher glass transition temperatures. We infer that methylation of the 8-quinolinol ligand reduces intermolecular interactions and consequently impedes charge transport through the film.

Introduction

Vacuum-deposited organic light-emitting device (OLED) technology has developed rapidly since the first report by Tang and Van Slyke of low voltage green electroluminescence (EL) from aluminum tris(8-quinolinolato) (Alq$_3$).[1] Since then, many other organic metal chelates have been demonstrated to be useful emitter materials or electron transporting hosts in dye-doped OLEDs.[2−5]

OLEDs are typically fabricated by vapor deposition of organic charge-transport and emitter materials on an indium tin oxide anode, followed by a low work function metal cathode. Many derivatives of Alq$_3$ have been investigated as emitter materials, including substitution of the metal ion with other trivalent metals (M^{+3} = Ga, In, and Sc)[5] and substitution of the 8-quinolinol ligand (substituent = F, Cl, NO_2[6], CN,[7] and alkyl[8,9] groups). More recently, Kido and Iisumi showed that aluminum tris(4-methyl-8-quinolinolato) (4Meq$_3$Al) exhibited a larger EL efficiency[10] than that of Alq$_3$.[1] This material was later shown to exhibit both a higher photoluminescence (PL) quantum efficiency than that of Alq$_3$ in solution and in the solid-state.[11] However, despite many experimental and theoretical studies of the archetypal Alq$_3$,[3] systematic analyses of the effects of small chemical changes are sparse and we lack a road map for improving on the overall EL device performance of Alq$_3$.

EL occurs when electrons and holes are injected and transported through the device where they form excitons near the organic heterojunction, which decay to give light emission. In dye-doped OLEDs, EL occurs by energy transfer from the host to the lower energy "guest" dye, which is usually incorporated by coevaporation.[4] In both types of devices, the design of efficient emitter materials and/or charge transporting hosts requires the optimization of several properties including (1) high PL efficiency, (2) sublimation without chemical degradation, (3) appropriate energy-level alignment with the cathode and hole-transport layer (HTL) for balanced charge injection and transport, and (4) the ability to form structurally stable films. These properties are strongly coupled to the

* To whom correspondence should be addressed.
† University of Nevada.
‡ Princeton University.
§ Present address: Pacific Northwest National Laboratories, Richland, WA 99352.

(1) Tang, C. W.; VanSlyke, S. A. *Appl. Phys. Lett.* **1987**, *51*, 913.
(2) Tang, C. W.; VanSlyke, S. A. *J. Appl. Phys.* **1989**, *65*, 3610.
(3) Chen, C. H.; Shi, J. *Coord. Chem. Rev.* **1998**, *171*, 161.
(4) Shoustikov, A. A.; You, Y.; Thompson, M. E. *IEEE J. Quantum Electron.* **1998**, *4(1)*, 3.
(5) Burrows, P. E.; Sapochak, L. S.; McCarty, D. M.; Forrest, S. R.; Thompson, M. E. *Appl. Phys. Lett.* **1994**, *64(20)*, 2718.
(6) Matsumura, M.; Akal, T. *Jpn. J. Appl. Phys.* **1996**, *35*, 5357.
(7) Burrows, P. E.; Shen, Z.; Bulovic, V.; McCarty, D. M.; Forrest, S. R.; Cronin, J. A.; Thompson, M. E. *J. Appl. Phys.* **1996**, *79(10)*, 7991.
(8) Hamada, Y.; Sano, M.; Fujita, T.; Nishio, Y.; Shibata, K. *Jpn. J. Appl. Phys.* **1993**, *32(4A)*, L514.
(9) Kido, J.; Iizumi, Y. *Chem. Lett.* **1997**, 963.
(10) Kido, J.; Iizumi, Y. *Appl. Phys. Lett.* **1998**, *73(19)*, 2721.
(11) Murata, H.; Merritt, C. D.; Mattoussi, H.; Kafafi, Z. H. *Proc. SPIE−Int. Soc. Opt. Eng.* **1998**, *3476*, 88.

10.1021/ja010120m CCC: $20.00
Published on Web 06/09/2001

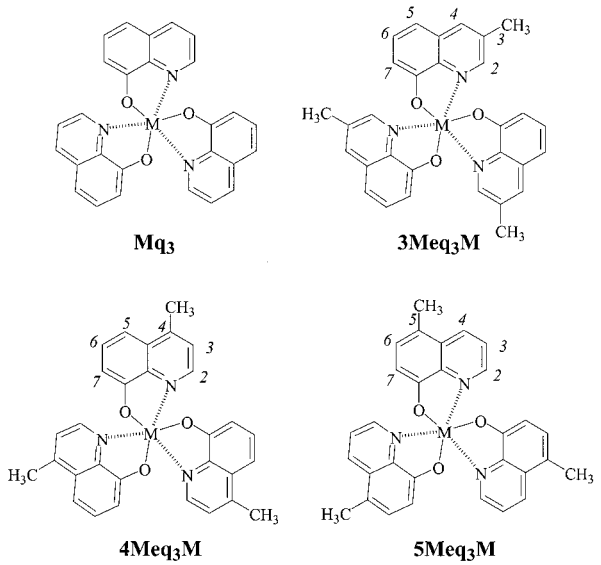

Figure 1. Metal (M = Al^{3+}, Ga^{3+}) tris(8-quinolinolato) chelates (*n*Meq_3M) used in this study.

molecular and electronic structure of the molecule, as well as the bulk packing of molecules achieved by vapor deposition.

In this paper, we present a study of the photoluminescent, electroluminescent, and thermal stability properties of aluminum and gallium tris(8-quinolinolato) (Mq_3; M^{+3} = Al, Ga) and their methyl-substituted derivatives, metal tris(4-methyl-8-quinolinolato) ($4Meq_3M$), tris(3-methyl-8-quinolinolato) ($3Meq_3M$), and tris(5-methyl-8-quinolinolato) ($5Meq_3M$; see Figure 1).

We show that methylation of the 8-quinolinol ligand decreases the crystalline melting point of the metal tris-chelates and increases the glass transition temperature of the amorphous materials compared to the unsubstituted analogues, in both cases indicative of reduced intermolecular interactions. In the case of the 3Meq and 4Meq ligands, we observe higher EL device operating voltages when the metal tris-chelates were used as the emitter material in OLEDs. We interpret this as evidence of a decreased overlap between the π-electron systems in the pyridyl rings of adjacent molecules, which is the site of the lowest unoccupied molecular orbital (LUMO) and, hence, the likely location of injected electrons. To our knowledge, this is the first established link between the electroluminescent and thermal (physical) properties of a series of electroluminescent compounds.

Experimental Section

Material Synthesis and Structural Characterization. All reagents, including Alq_3 used as the reference material in these studies were obtained from Aldrich Chemical Co. The ligands 3Meq and 4Meq were synthesized by the Doebner-Von Miller reaction starting with the appropriately substituted *o*-aminophenol and unsaturated aldehyde or ketone.[12] After extraction of the reaction mixture, the ligands were isolated in low yields (30%). The 5Meq ligand was prepared in higher yields (57%) by electrophilic substitution of 8-quinolinol with formaldehyde and hydrochloric acid followed by reductive catalytic hydrogenation.[13] All ligands were purified by sublimation. The metal tris-chelates were prepared by combining either $AlCl_3$ or $Ga(NO_3)_3$ hexahydrate salt and the appropriate ligand in a 1:3 molar ratio in aqueous solution buffered with ammonium acetate.[14] The crude materials were recrystallized from methanol with the exception of the 4MeqM chelates. These materials exhibited extremely high solubility in most common recrystallization solvents and precluded the practicality of purification by recrystallization. However, all materials were purified by high-vacuum gradient-temperature sublimation[15] before analysis. Structures of all materials were confirmed by ^1H NMR spectroscopy reported elsewhere[16] and elemental analysis obtained from Nu Mega Resonances Lab, Inc. Spectroscopic data for the ligands and *n*Meq_3M chelates match those previously reported.[14]

Thermal Stability Characterization. Thermal analysis was determined by differential scanning calorimetry (DSC) and thermal gravimetric analysis (TGA) performed simultaneously using a Netzsch simultaneous thermal analyzer (STA) system. Pure polycrystalline samples (5−10 mg) were placed in aluminum pans and run at a rate of 20 °C/min under N_2 gas at a flow rate of 50 mL/min. The temperatures of phase transitions were measured including the crystalline melting point (T_m). Indium metal was used as the temperature standard. The melted samples were cooled rapidly or by a controlled cooling rate of 20 °C/min to form glasses. The glass transition (T_g) and the crystallization point (T_{c1}) were measured from a second heating of the glassy state. The maximum weight loss temperature (decomposition temperature) was determined for each sample run without a lid and reported as the maximum peak of the DTGA (derivative of the TGA curve).

Electronic Characterization. Absorption and photoluminescence characterization were performed on dilute ($\sim 10^{-5}$ M) dimethyl formamide (DMF) and methylene chloride (CH_2Cl_2) solutions. Absorption spectra were recorded with a Varian Cary 3Bio UV−vis spectrophotometer, and PL spectra were obtained with a SLM 48000 spectrofluorimeter. Relative PL quantum efficiencies (ϕ_{PL}) were determined from degassed DMF solutions by adjusting the concentration of the sample so that the optical densities at 390 nm (excitation wavelength) were <0.2 absorption units. PL quantum yields were calculated relative to the known value for Alq_3 in DMF ($\phi_{PL} = 0.116$)[17] and are reported normalized to Alq_3.

Electroluminescence Characterization. Organic light-emitting devices (OLEDs) were fabricated using each of the *n*Meq_3M chelates as the emissive layer. Devices were grown on glass slides precoated with indium tin oxide (ITO) with a sheet resistance of 15 Ω/square. The ITO substrates were degreased in detergent and then boiled in 1,1,1-trichloroethane, rinsed with reagent grade acetone, and finally rinsed with methanol before being dried in a stream of pure nitrogen. The substrates were exposed to UV−ozone for 5 min before being loaded into a nitrogen glovebox coupled to the vacuum system. A 500 Å thick layer of the preferentially hole transporting material, *N*,*N*′-diphenyl-*N*,*N*′-bis(3-methylphenyl)1,1′-biphenyl-4,4′-diamine (TPD) or *N*,*N*′-diphenyl-*N*,*N*′-bis(1-naphthol)1,1′-biphenyl-4,4′diamine (α-NPD), was deposited on the ITO substrate by thermal evaporation from a baffled Mo crucible at a nominal rate of 2−4 Å/s under a base pressure of $<2 \times 10^{-6}$ Torr. A 550 Å thick layer of the preferentially electron-transporting (ETL) metal tris(8-quinolinolato) chelates, also serving as the emitter layer (EML), were then deposited on the HTL. A top electrode consisting of circular 1 mm diameter contacts was subsequently deposited by thermal evaporation through a shadow mask. Two different types of cathodes were utilized, LiF/Al and a Mg:Ag alloy. The LiF/Al cathode consisted of a 5 Å LiF layer deposited on the EML followed by a 1000 Å layer of Al metal. For the Mg:Ag cathode, a Mg:Ag alloy layer (1000 Å) was deposited by coevaporation of the two metals from separate Ta boats in a 10:1 Mg:Ag atomic ratio under a base pressure of 10^{-5} Torr, followed by a 300 Å Ag cap. For the systematic study, all HTL and cathode layers were deposited simultaneously and the devices were never exposed to air during fabrication. Thus, devices produced from different metal chelate materials were identical in all respects. A quartz crystal oscillator placed near the substrate was used to measure the thickness of the films. Film thickness calibration was performed by ellipsometry of films grown on silicon.

Devices were tested in air with an electrical pressure contact made

(12) Utermohlen, W. P. *J. Org. Chem.* **1943**, *8*, 544.
(13) Buckhalter, J. H.; Ceib, R. I. *J. Am. Chem. Soc.* **1961**, *26*, 4078.
(14) Schmidbaur, H.; Lattenbauer, J.; Dallas, L.; Muller, W. G.; Kumberger, O. *Z. Naturforsh.* **1991**, *46B*, 901.
(15) Forrest, S. R.; Kaplan, M. L.; Schmidt, P. H. *Annu. Rev. Mater. Sci.* **1987**, *17*, 189.
(16) Padmaperuma, A. M.S. Thesis in Chemistry, University of Nevada, Las Vegas, 2000.
(17) Lytle, F. E.; Story, D. R.; Juricich, M. E. *Spectrochim. Acta*. **1973**, *29A*, 1357.

Table 1. Thermal Analysis Data

metal chelate	T_m (°C)	ΔH_{fusion} (kJ/mol)[a]	T_g (°C)[b]	T_{c1} onset (°C)[b]	max. wt. loss temp. (°C)
Alq_3	419	n.d.	177	251	487
$3Meq_3Al$	406	n.d.	n.o.	n.o.	465
$4Meq_3Al$	345	43.0	194	n.o.	494
$5Meq_3Al$	401	53.2	198	n.o.	495
Gaq_3	409	n.d.	n.o.	244	472
$3Meq_3Ga$	414	56.7	204	269	454
$4Meq_3Ga$	352	40.8	192	n.o.	473
$5Meq_3Ga$	407	52.9	202	n.o.	480

[a] n.d. = not determined because of overlapping peaks. [b] n.o. = not observable.

by means of a 25 μm diameter Au wire. Current−voltage characteristics were measured with a Hewlett-Packard HP4145 semiconductor parameter analyzer, and the EL intensity was measured with a Newport 835 optical power meter with a large area photodetector placed directly below the glass substrate. Thus, all efficiencies reported are measured directly from the back of the device with no corrections or assumptions regarding the angular dependence of the EL or the relationship between luminance and quantum efficiency.[10] Spectra were recorded with an EG&G optical multichannel analyzer on a 0.25 focal length spectrograph.

Results

Thermal Stability. The morphological stability of Alq_3, desirable for practical OLED applications, has been attributed to its intrinsic polymorphic, racemic nature, and strong dipolar interactions[18] giving rise to a high T_g (175 °C).[19] The thermal properties of Alq_3 and Gaq_3 and their methyl-substituted derivatives were evaluated by simultaneous thermal analysis (STA), where TGA and DSC experiments were run simultaneously; therefore, thermal events observed in DSC can be directly correlated with weight loss events. Results are presented in Table 1.

Several phase transitions were observed for Alq_3 in addition to a large melting transition (T_m) at 419 °C. A small broad transition beginning at 320 °C and a coupled endotherm (393 °C) and exotherm (396 °C) were observed prior to T_m. These additional phase transitions are attributed to polymorphism of the crystalline material as discussed by Brinkmann[18] and were nearly unobservable at a slower heating rate (5 °C/min). The thermal transitions were accompanied by a ~15% weight loss measured immediately following T_m (endpoint = 422 °C). This weight loss is attributed to sublimation of the sample, which occurs simultaneously with melting of the different polymorphic phases. This is supported by Brinkman's assignment of the exothermic transition observed by DSC (see Figure 3a) as a phase transition from α-Alq_3 to the γ-Alq_3 phase at ~395 °C, where further heating of the material (>410 °C) was shown to result in sublimation (ΔH = 49 kJ/mol) of the α-Alq_3 phase, confirmed by X-ray diffraction. We observed similar thermal behavior for Alq_3 and, thus, strongly believe that the nature of the ~15% weight loss was due to sublimation. Furthermore, when stopping the thermal experiment just past the major endothermic transition (T_m) a film was observed on the inside lid of the sample pan for all materials studied. The material left in the pan was analyzed by ^{1}H NMR and FT-IR, and no decomposition products were observable by those techniques. In a separate experiment, DTGA, and thus percent weight loss, was determined without a lid and no attempt to analyze the evolved species after the major weight loss (DTGA) was conducted.

All metal tris(8-quinolinolato) materials in our study exhibited similar weight loss behavior, where the magnitude of the weight loss was independent of metal ion substitution but dependent on the position of methylation of the ligand. Further heating to 500 °C resulted in decomposition of the samples.

Upon methyl substitution of Alq_3, T_m increases in the order $4Meq_3Al \ll 3Meq_3Al \sim 5Meq_3Al < Alq_3$, and for the gallium chelate series, $4Meq_3Ga \ll 5Meq_3Ga < Gaq_3 < 3Meq_3Ga$. In addition, multiple phase transitions similar to Alq_3 were observed for Gaq_3 and $3Meq_3Al$, suggesting that these materials also exhibit polymorphism (see Figure 2). Although crystalline melting points of the Mq_3 chelates are lowered upon methylation, the thermal decomposition temperatures were higher than the unsubstituted analogues with the exception of the $3Meq_3M$ chelates. The trend in thermal decomposition temperatures were similar for both metal chelate series, with stability increasing in the order $3Meq_3M < Mq_3 < 4Meq_3M < 5Meq_3M$.

The glassy state of Alq_3 was difficult to form as discussed by Naito[19] but was achieved by cooling at a rate of 20 °C/min of the crystalline material immediately following the melting transition in the first heating cycle. A second heating cycle of Alq_3 revealed a glass transition (T_g) at 177 °C and a recrystallization exotherm (T_{c1}) at 251 °C, followed by melting. These values are slightly higher than previously reported[19] because of the faster heating rate used here. Glass formation was also difficult for Gaq_3 and $3Meq_3Al$, preventing determination of T_g. However, $3Meq_3Ga$ and the $4Meq_3M$ and $5Meq_3M$ chelates formed glasses facilely and showed 15−20 °C higher T_g than that of Alq_3. A comparison of the second heating cycles for Alq_3 and $4Meq_3Al$ glasses is shown in Figure 3. Unlike Alq_3, the $4Meq_3M$ and $5Meq_3M$ chelates showed no recrystallization of the glassy state even after heating beyond T_g and up to decomposition near 500 °C. This suggests that the entropic difference between the crystalline and amorphous states is smaller for the C-4 and C-5 methylated derivatives compared to those of the C-3 methylated and unsubstituted analogues.

Electronic Properties. The optical transition responsible for photoluminescence in metal (8-quinolinolato) chelates is centered on the organic ligand. This transition is due to a $\pi-\pi^*$ charge transfer from the electron rich phenoxide ring (location of the highest occupied molecular orbital, or HOMO) to the electron deficient pyridyl ring (location of the LUMO).[20] Therefore, as reported previously,[3] substitution of an electron donating group on the pyridyl ring raises the energy of the LUMO and on the phenoxide ring raises the energy of the HOMO, resulting in a blue and red-shift of the absorption energies, respectively. The absorption spectra of the nMeq$_3$M chelates in DMF are shown in Figure 4. Upon methyl substitution (weakly electron donating) of aluminum tris(8-quinolinolato), the absorption energy shifts were largest for C-5 methylation of the phenoxide ring (red-shift, >1000 cm^{-1}) and very small for C-3 and C-4 methylation of the pyridyl ring (blue-shift, < 350 cm^{-1}). Substitution of the heavier metal ion Ga causes a red-shift of absorption compared to those of the nMeq$_3$Al chelates because of the heavy atom effect discussed previously,[5] but the trends in absorption shifts upon methylation of the 8-quinolinol ligand were identical to those of the aluminum series. The polarity of the solvent had almost no effect on absorption energies as shown in Table 2 for CH_2Cl_2 and Table 3 for the more polar DMF solvent.

(18) Brinkmann, M.; Gadret, G.; Muccini, M.; Taliani, C.; Masciocchi, N.; Sironi, A. *J. Am. Chem. Soc.* **2000**, *122*, 5147.
(19) Naito, K.; Muira, *J. Phys. Chem.* **1993**, *97*, 6240.
(20) Curioni, A.; Boero, M.; Andreoni, W. *Chem. Phys. Lett.* **1998**, *294*, 263.

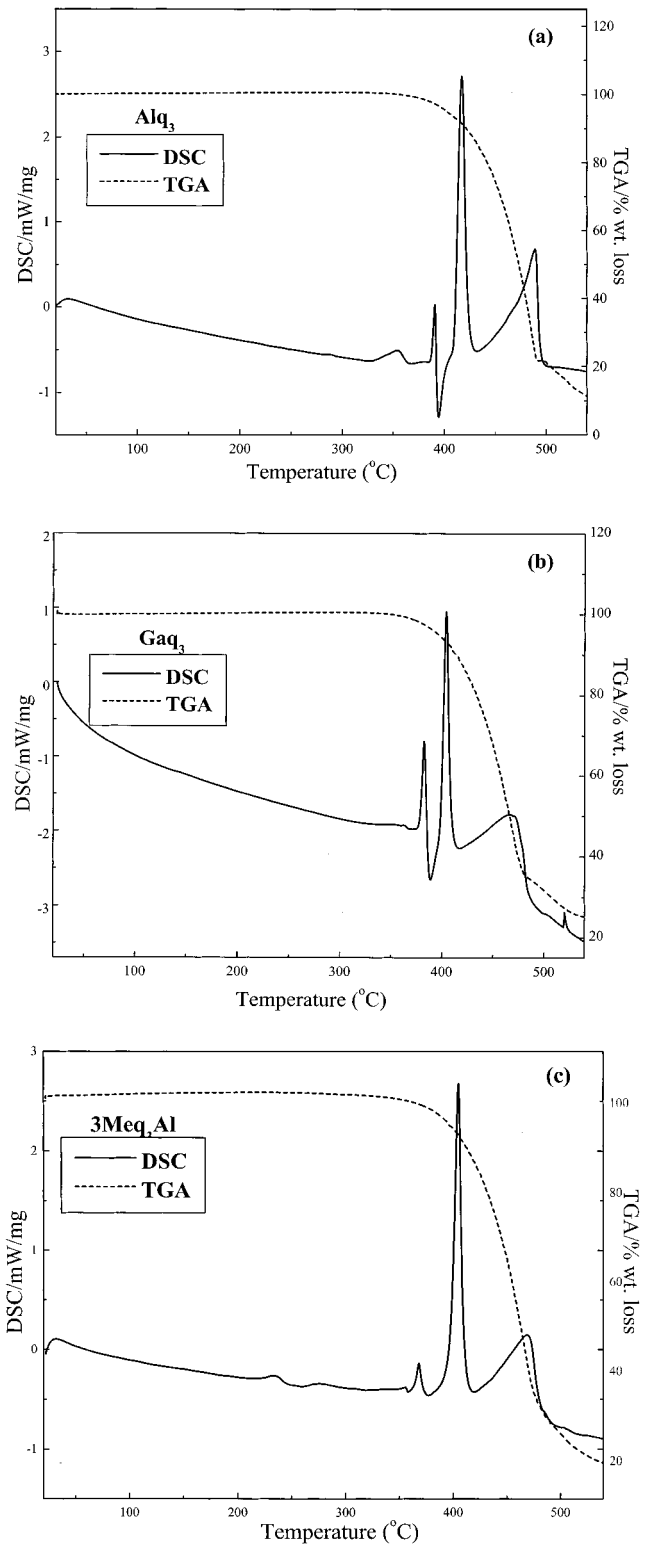

Figure 2. DSC and TGA traces of metal tris(8-quinolinolato) chelates showing multiple thermal transitions (°C): (a) Alq_3, 354, 393, 396 (exotherm), 419; (b) Gaq_3, 369, 387, 396 (exotherm), 409; and (c) $3Meq_3Al$, 233, 275, 355, 358 (exotherm), 370, 377 (exotherm), 406.

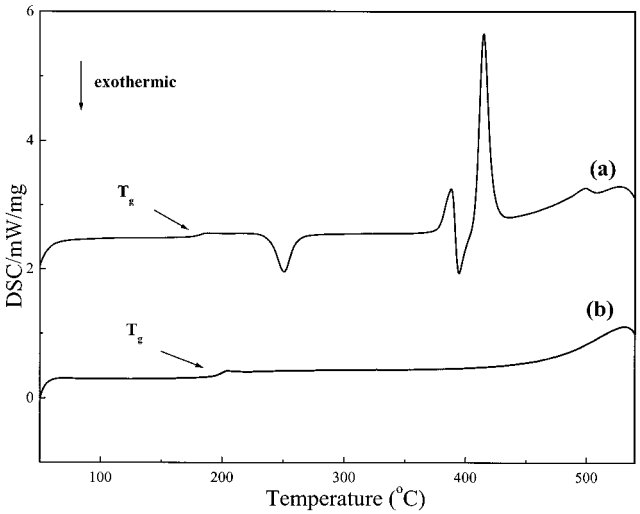

Figure 3. DSC traces of the second heating after melting and controlled cooling to the glassy state for (a) Alq_3 and (b) $4Meq_3Al$ showing T_g's of 177 and 194 °C, respectively.

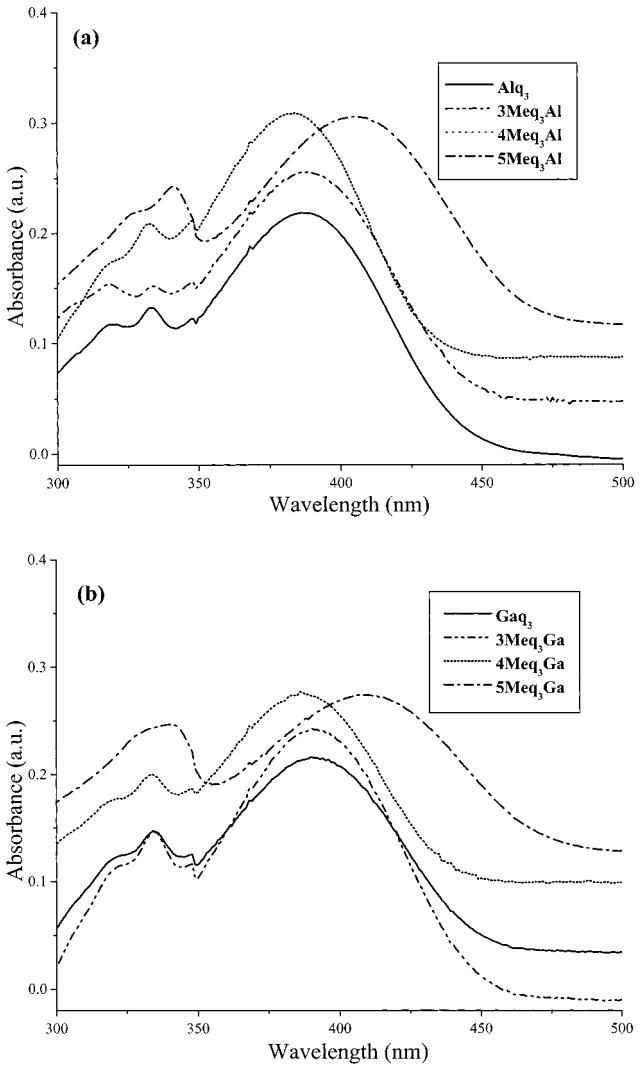

Figure 4. Absorption spectra run in DMF showing the energy shifts upon methylation of the ligand for (a) *n*Meq_3Al and (b) *n*Meq_3Ga chelates.

Figure 5 shows the photoluminescence (PL) spectra obtained in DMF solution. The effect of methyl substitution on the PL emission energies were similar to those observed for absorption. The Franck−Condon (F−C) shifts (energy difference between absorption and emission maxima; Δ) and the fwhm of emission are also reported. The smallest F−C shifts and the narrowest fwhm were observed for $4Meq_3Al$ (5912 cm^{-1}) and $4Meq_3Ga$ (6280 cm^{-1}) compared to those of the unsubstituted analogues Alq_3 (6623 cm^{-1}) and Gaq_3 (7026 cm^{-1}).

Table 2. Photophysical Data in CH_2Cl_2 Solution

metal chelate	abs. CH_2Cl_2 λ_{max} (nm)	abs. energy shift from Mq_3 (cm^{-1})	emission CH_2Cl_2 λ_{max} (nm)	emission energy shift from Mq_3 (cm^{-1})	fwhm (nm)	Δ (cm^{-1})
Alq_3	388		514		102	6318
$3Meq_3Al$	386	+133	520	−224	92	6776
$4Meq_3Al$	381	+473	495	+747	92	6045
$5Meq_3Al$	405	−1082	547	−1174	109	6410
Gaq_3	392		543		110	7162
$3Meq_3Ga$	386	+396	540	+102	110	7388
$4Meq_3Ga$	385	+464	514	+1039	102	6519
$5Meq_3Ga$	408	−1000	568	−810	112	6904

The PL quantum yields are reported relative to the known quantum yield for Alq_3 in DMF and normalized to $\phi_{PL}(Alq_3) = 1.00$ for clarity in Table 3. The highest ϕ_{PL} is exhibited by $4Meq_3Al$ (3 times Alq_3). This is higher than those in reports by Murata et al.[11] in $CHCl_3$ (2 times Alq_3) and in the solid-state (1.6 times Alq_3). The higher polarity of the DMF solvent enhances the quantum efficiency more for $4Meq_3Al$ relative to Alq_3 but has almost no effect on the PL λ_{max} which is similar to that reported by Kido and Iizumi for the solid-state film.[10] The $3Meq_3Al$ chelate also showed an increase in ϕ_{PL} compared to Alq_3 but of smaller magnitude, whereas the $5Meq_3Al$ derivative exhibited a significant decrease in PL quantum efficiency (approximately 3 times less than that of Alq_3). The same trends in PL efficiencies upon methyl substitution were observed when Al was replaced with Ga but with a corresponding 4 times decrease in ϕ_{PL} as shown previously for Gaq_3.[5,21] In general, methylation of the pyridyl ring enhances ϕ_{PL} and methylation of the phenoxide ring decreases it.

We speculate that the large enhancement in ϕ_{PL} by C-4 methylation of Al and Ga tris (8-quinolinolato) chelates is due to reduced energy loss in the excited-state vibrational manifold, as indicated by the smaller Δ's and narrower fwhm's. This is supported by a recent study of the infrared absorption and photoluminescence of matrix-isolated and thin-film samples of Alq_3 and $4Meq_3Al$ compared to vibrational spectra based on density functional calculations.[22] There, the PL spectra of matrix-isolated molecules revealed vibronic bands characterized as a combination of ring breathing and metal−ligand stretching modes. Kushto et al. noted that there was a lack of metal−ligand character in the vibrations of $4Meq_3Al$ as compared to Alq_3, suggesting that the stronger coupling of the metal−ligand stretching coordinates to the electronic transition in Alq_3 may provide additional paths for nonradiative decay that are not available to $4Meq_3Al$, giving rise to a higher ϕ_{PL} for the latter.

Electroluminescence Properties. EL spectra are shown in Figure 6. The EL emission energy shifts are consistent with those observed in the PL spectra. However, the $5Meq_3Ga$ gave rise to an additional lower energy peak in the EL spectrum that was not observed in the solution PL spectrum (Figure 6b). The origin of this peak has not been elucidated but was observed as a very weak shoulder in the PL spectrum of a vapor-deposited film, thus excluding the origin due to exciplex formation at the interface with the HTL material as reported for other materials.[23] However, this does not exclude the possibility of excimer formation, which may be one of the reasons for the substantially lower PL quantum efficiencies for the C-5 methylated derivatives. The EL emission spectrum for the $3Meq_3Al$ derivative is not shown but was identical to that of Alq_3.

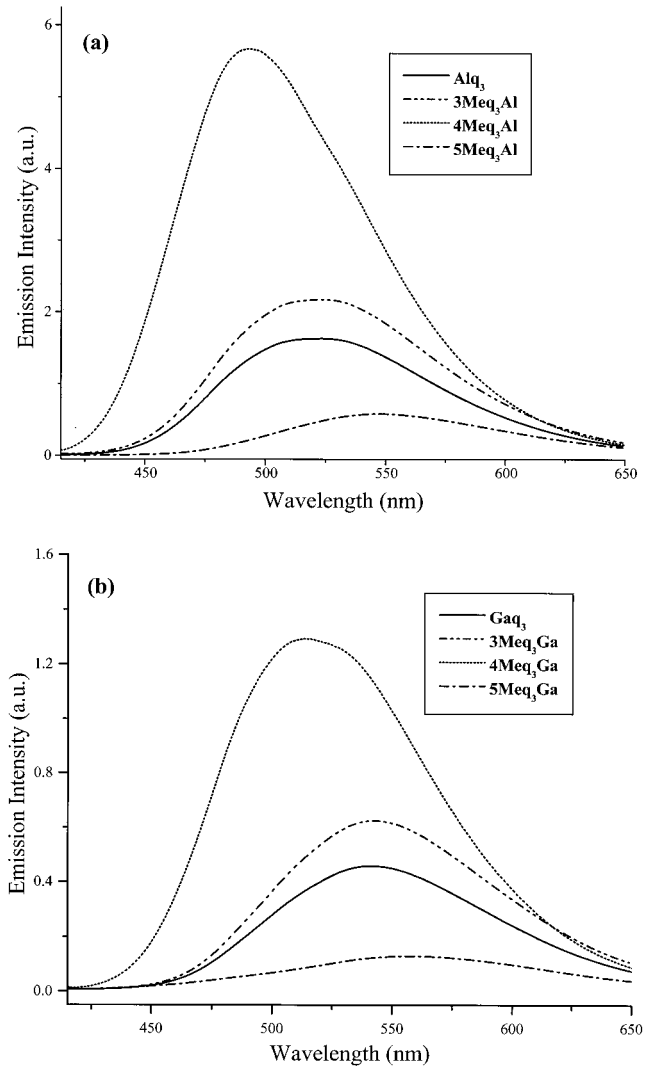

Figure 5. Photoluminescence spectra run in DMF for (a) nMeq$_3$Al and (b) nMeq$_3$Ga chelates.

The current versus voltage characteristics of OLEDs composed of ITO/NPD/nMeq$_3$M/LiF−Al are shown in Figure 7. The device operating voltages (at a fixed current) increases in the order $Mq_3 < 5Meq_3M < 4Meq_3M$ for both aluminum and gallium tris-chelates. Figure 8 shows the dependence of the optical output power on drive current for each of the OLEDs. At a current of 100μA, the EL output increases in the order $5Meq_3M < Mq_3 < 4Meq_3M$. Identical devices prepared with a Mg:Ag cathode gave similar results with the exception of $4Meq_3Ga$ which required a lower voltage compared to that of $5Meq_3Ga$.

The EL efficiencies (ϕ_{EL}) relative to $Alq_3 = 1.0$ are reported in Table 4. For both series of nMeq$_3$M chelates, the C-4 methylated derivatives exhibited the highest efficiencies. $4Meq_3Al$ and $4Meq_3Ga$ showed approximately a 1.4 times increase in η_{EL} compared to Alq_3 and Gaq_3 respectively, for both types of cathodes utilized. However, the η_{EL} for $4Meq_3Al$ was smaller than previously reported for a similar device using TPD as the HTL and Mg:Ag as the cathode.[9,10] Therefore, a second series of devices were prepared by varying the HTL (α-NPD versus

(21) Sapochak, L. S.; Burrows, P. E.; Garbuzov, D.; Ho, D. M.; Forrest, S. R.; Thompson, M. E. *J. Phys. Chem.* **1996**, *100*, 17766.

(22) Kushto, G. P.; Iizumi, Y.; Kido, J.; Kafafi, Z. H. *J. Phys. Chem. A* **2000**, *104*, 3670.

(23) Ogawa, H.; Okuda, R.; Shirota, Y. *Mol. Cryst. Liq. Cryst. Sci. Technol.* **1998**, *315*, M489.

Table 3. Photophysical Data in DMF Solution

metal chelate	abs. DMF λ_{max} (nm)	abs. energy shift from Mq_3 (cm^{-1})	emission DMF λ_{max} (nm)	emission energy shift from Mq_3 (cm^{-1})	fwhm (nm)	Δ (cm^{-1})	relative ϕ_{PL} (Alq_3 =1.0)
Alq_3	388		521		105	6623	1.0
$3Meq_3Al$	387	+66	521	0	106	6668	1.4
$4Meq_3Al$	383	+336	494	+1049	92	5912	3.0
$5Meq_3Al$	405	−1082	546	−879	113	6376	0.29
Gaq_3	392		541		110	7026	0.28
$3Meq_3Ga$	392	0	543	−68	111	7094	0.38
$4Meq_3Ga$	388	+263	513	+1009	103	6280	0.79
$5Meq_3Ga$	409	−1060	558	−563	119	6529	0.08

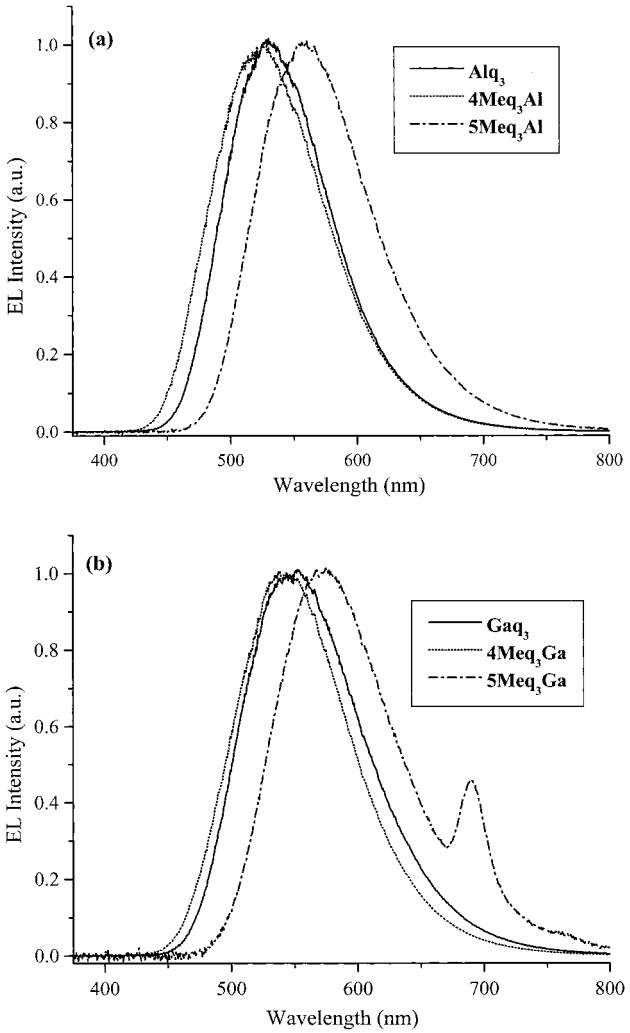

Figure 6. EL spectra obtained from LiF−Al/nMeq_3M/NPD OLEDs for (a) *n*Meq_3Al and (b) *n*Meq_3Ga chelates.

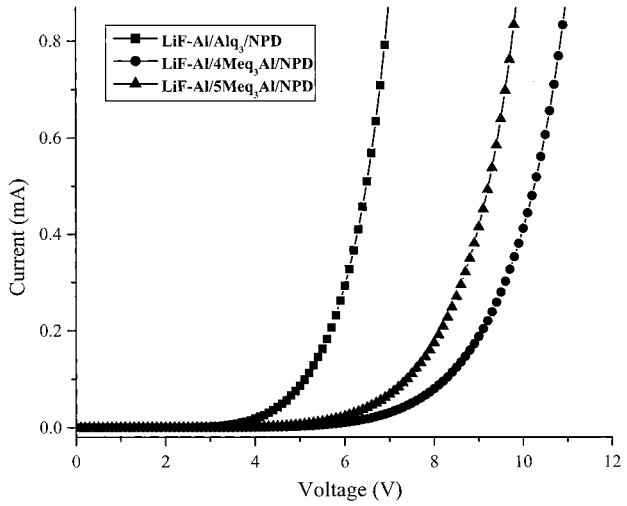

Figure 7. Current vs voltages plots for Alq_3, $4Meq_3Al$, and $5Meq_3Al$ OLEDs.

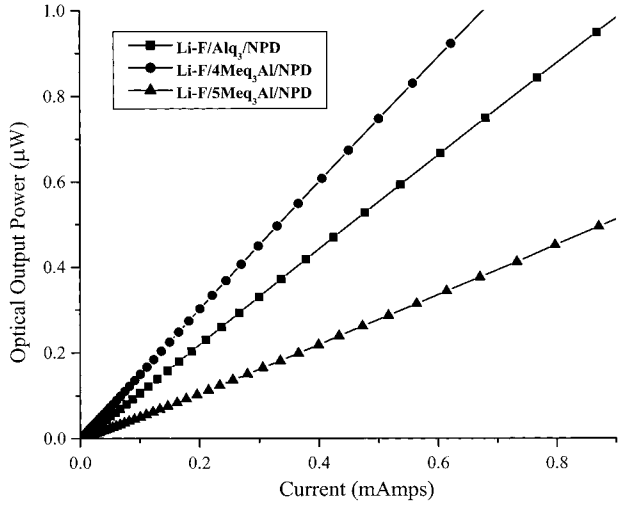

Figure 8. Light output vs current plots for Alq_3, $4Meq_3Al$, and $5Meq_3$-Al OLEDs.

TPD) with the *n*Meq_3Al chelates as the emitter material and Mg:Ag as cathode. Results are shown in Table 5. In general, we observed similar trends in η_{EL} with a slightly higher efficiency for TPD-based devices because of better energy level alignment at the ETL/HTL interface. The voltage trend did not change with the composition of the HTL, suggesting that the source of higher voltages (and hence the overall lower emission power efficiencies) for the methylated derivatives is mainly due to reduced charge transport efficiency of these latter compounds as compared to that of Alq_3.

Discussion

The differences in EL performance of the *n*Meq_3M chelates in this study can be related to the changes in material properties caused by methylation of the ligand. The substantially larger PL efficiencies for C-4 methylated derivatives contributed to their larger η_{EL}. However, for all methylated derivatives, if charge injection and transport were similar and ϕ_{PL} was the dominating factor for high EL efficiencies, then the ratio of relative EL and PL efficiencies (η_{EL}/ϕ_{PL}) should all be close to 1.0. However, this ratio is <1.0 for $4Meq_3Al$ and $3Meq_3Al$ but >1.0 for $5Meq_3Al$. For the gallium series, all ratios are >1.0 with $4Meq_3Ga$ showing the smallest value. This suggests that charge injection and/or transport efficiencies are not the same for these materials and are reduced by methylation of the pyridyl ring for both Alq_3 and Gaq_3, compared to the other methylated

Table 4. EL Device Data Utilizing Different Cathodes

	LiF−Al/EML/NPD device			Mg:Ag/EML/NPD device		
EML	η_{EL} (Alq_3=1.0)	voltage (at 13mA/cm^2)	η_{EL}/ϕ_{PL} (Alq_3=1.0)	η_{EL} (Alq_3=1.0)	voltage (at 13mA/cm^2)	η_{EL}/ϕ_{PL} (Alq_3=1.0)
Alq_3	1.0	5.3	1.0	1.0	5.6	1.0
$4Meq_3Al$	1.4	7.8	0.47	1.3	8.2	0.45
$5Meq_3Al$	0.45	7.4	1.5	0.49	7.3	1.7
Gaq_3	0.63	5.7	2.2	0.65	6.4	2.3
$4Meq_3Ga$	1.0	7.6	1.3	0.97	6.5	1.2
$5Meq_3Ga$	0.21	5.8	2.6	0.24	8.0	3.0

Table 5. EL Device Data Utilizing Different HTLs

EML/ HTL	voltage (at 13 mA/cm^2)	η_{EL} (Alq_3/NPD = 1.0)	η_{EL}/ϕ_{PL} (Alq_3/NPD = 1.0)
Alq_3/NPD	6.3	1.0	1.0
$3Meq_3Al$/NPD	7.2	0.80	0.64
$4Meq_3Al$/NPD	7.1	1.2	0.40
$5Meq_3Al$/NPD	6.9	0.39	1.3
Alq_3/TPD	7.1	1.1	1.1
$4Meq_3Al$/TPD	7.7	1.6	0.52
$5Meq_3Al$/TPD	6.2	0.48	1.7

derivatives, but less so for the latter. This is consistent with the need for higher operating voltages for OLEDs utilizing $4Meq_3$-Al and $3Meq_3Al$.

Because methylation of the pyridyl ring (C-3 or C-4 positions) causes only very small shifts in the absorption energy and thus does not significantly shift the energy of either the HOMO or LUMO compared to those of the unsubstituted analogues, it seems likely that the energy level matching with the metal cathode and HTL are similar to the unsubstituted analogues. As a result, charge-injection efficiency is unlikely to be significantly affected by C-4 or C-3 methylation, and indeed, we observe power law, interface limited charge transport in all cases.[24] Therefore, the reason for the higher operating voltages is due to poorer electron transport through the metal/organic interface region.

The efficiency of charge-transport in organic molecular crystals is enhanced by strong intermolecular interactions of the polarizable π-system and is dependent on the molecular packing in the solid-state. Although vapor-deposited films of Alq_3 and Gaq_3 are amorphous, crystallographic data for single crystals provides important information about their molecular packing preferences. For example, Alq_3 and Gaq_3 show strong dipolar $\pi-\pi$ stacking interactions (3.5−3.9 Å) of the 8-quinolinol ligands between adjacent molecules with preferential overlap of the pyridyl rings.[14,18,25] Because the pyridyl ring is the location of the LUMO, this explains the higher electron verses hole mobility in Alq_3 and related metal(8-quinolinolato) chelates. Additionally, hydrogen-bonding interactions between the phenolic oxygen with H-atoms at the C-5 and C-4 positions on adjacent molecules have been identified for Gaq_3.[25] Therefore, it is not unexpected that a decrease in $\pi-\pi$ stacking due to steric factors, changes in polarity (via changes in the dipole moment of the ligand),[26] as well as loss of hydrogen-bonding interactions of the metal chelates will result upon methylation of the 8-quinolinol ligand. These changes will reduce the cohesive forces between molecules, and analysis of the series of methyl-substituted derivatives by thermal analysis reveals these differences.

Thermal analysis showed that the $4Meq_3M$ chelates exhibited the lowest (∼60 °C) melting points and smaller enthalpies of fusion (ΔH_{fus}) of the series, also clearly indicative of weaker intermolecular interactions. Glass transition temperatures were ∼20 °C higher than those of the unsubstituted analogues with no recrystallization of the amorphous state, suggesting that the entropic difference between the crystalline and amorphous states is small compared to that of Mq_3 materials. These differences in thermal properties result because C-4 methyl substitution of the ligand acts to eliminate one of the H-bonding interactions, as well as decrease the overlap between pyridyl rings of adjacent molecules. Although methyl substitution at the C-3 position could also act to prevent efficient overlap of pyridyl rings, the C-4 and C-5 positions of $3Meq_3M$ chelates are still available for H-bonding interactions. The $3Meq_3M$ chelates do not show a significantly lower crystalline melting point and do not form stable glasses. For both $4Meq_3M$ and $3Meq_3M$ chelates, therefore, a decrease in pyridyl ring overlap leads to inefficient electron transport properties because the pyridyl ring of the 8-quinolinol ligand is the site of the LUMO and, hence, the location of injected electrons. This is the likely source of the higher operating voltages exhibited by $4Meq_3Al$- and $3Meq_3$-Al-based OLEDs.

The device operating voltage for $5Meq_3Al$ was also increased compared to that of Alq_3 but less so than the 3- and $4Meq_3Al$ chelates. The crystalline melting point of $5Meq_3Al$ was slightly lower than those of $3Meq_3Al$ and Alq_3, but it exhibits a high glass transition temperature with no recrystallization of the amorphous state similar to that of $4Meq_3Al$. C-5 methylation of the phenoxide ring will also result in decreased $\pi-\pi$ stacking compared to that of Alq_3 with loss of the C-5 H-bonding interaction but will not prevent preferential overlap of the pyridyl rings. Furthermore, unlike the $4Meq_3M$ and $3Meq_3M$ chelates, in an OLED, hole-injection may be improved because the HOMO energy of Alq_3 is raised on C-5 methylation, and therefore, $5Meq_3Al$ may also have closer energy level alignment with the HOMO of the HTL. We speculate, therefore, that both charge transport and hole injection efficiencies may be higher in $5Meq_3Al$ OLEDs explaining why η_{EL}/ϕ_{PL} is much larger for $5Meq_3Al$ compared to those of $4Meq_3Al$ and $3Meq_3Al$.

The effect of methylation of Gaq_3 on the thermal properties was similar to that of the aluminum series. However, the EL properties cannot be explained in the same manner as those of Alq_3 and its methylated derivatives. Although the gallium series exhibited an approximately four times decrease in relative PL quantum efficiencies compared to those of the nMeq$_3$Al analogues, η_{EL}/ϕ_{PL} ratios are substantially larger for all nMeq$_3$-Ga chelates. The gallium series are red-shifted in absorption energy compared to that of the aluminum chelate analogues because of a higher HOMO energy resulting in improved energy level alignment and more efficient hole injection at the HTL/nMeq$_3$Ga interface. Because the operating voltage is dependent on both charge injection and charge transport efficiencies, the

(24) Baldo, M. A.; Forrest, S. R. *10th Int. Workshop on Inorganic and Organic Electroluminescence (EL'00)*; Hamazuatsu, Dec 4−7, 2000; Paper Mo-08, p 53.

(25) Wang, Y.; Zhang, W.; Li, Y.; Ye, L.; Yang, G. *Chem. Mater.* **1999**, *11*, 530.

(26) Bader, M. *J. Am. Chem. Soc.* **1992**, *114*, 6575.

enhancement of the former may outweigh the effects of reduced charge transport caused by methylation of the ligand.

We are currently investigating the effect of methylation of zinc bis(8-quinolinolato) chelate materials. In those materials, the trends in absorption and emission energy shifts, PL quantum efficiencies, and thermal properties upon methyl substitution are similar to those of the tris-chelate series. This suggests that the dipolar interaction and preferential overlap of pyridyl rings of adjacent molecules may be similar for the tetracoordinate zinc bis-chelates, and therefore, similar trends in EL device characterization are expected.

One way to test if preferential overlap of pyridyl rings is important for electron transport in metal (8-quinolinolato) chelate materials is to compare the effect substituents with different geometries have on the resulting EL properties. For example, comparison of metal (8-quinolinolato) derivatives with C-4 substitution of the ligand with a trifluoromethyl group, having approximately tetrahedral geometry, versus a cyano group with linear geometry will result in different bulk packing characteristics. It is expected that the linear cyano group will be less prone to preventing overlap of pyridyl rings and, thus, should not inhibit charge transport. However, unlike the methyl group, both the trifluoromethyl and cyano groups are strongly electron withdrawing, which will cause a lowering of the LUMO energy of resulting metal (8-quinolinolato) chelates. Therefore, the resulting EL efficiencies will also depend on how the C-4 substitution influences the HOMO−LUMO overlap within the ligand itself.

Conclusions

A systematic study of the effect of methylation of aluminum and gallium tris(8-quinolinolato) chelates on the PL, EL, and thermal properties was presented. We showed that, although ϕ_{PL} and η_{EL} were increased by C-4 methylation of the 8-quinolinol ligand for both series of metal chelates, a higher device operating voltage was required because of a decrease in pyridyl ring overlap, thus leading to poorer electron transport efficiency. These results were explained by correlating the thermal properties of the methylated metal tris-chelates and the OLED device performance characteristics. Our results suggest that it may be possible to improve overall EL efficiency of metal tris(quinolinolato) chelates by a judicious choice of both the type of substituent group and the position on the 8-quinolinol ligand in order to achieve a balance between high ϕ_{PL}, charge injection efficiency, and charge transport ability. The conclusions drawn from the thermal analysis data are important for understanding how methylation affects the physical properties of the metal chelates. However, such an interpretation is only valid when comparing a series of chemically similar compounds, where similar comparisons of unrelated materials would not be as useful.

Acknowledgment. The authors gratefully acknowledge NSF (DMR-9874765 Grant), Research Corporation, DOE, DARPA, AFOSR, and Universal Display Corporation for financial support of this research.

JA010120M